Single-Crystal Particles of Mesoporous Niobium−Tantalum Mixed Oxide

Byongjin Lee,† Tomohiro Yamashita,† Daling Lu,‡ Junko N. Kondo,† and Kazunari Domen*,‡

Chemical Resources Laboratory, Tokyo Institute of Technology,4259 Nagatsuta-cho, Midori-ku, Yokohama, 226-8503, Japan, and Core Research for Evolutional Science and Technology, Japan Science and Technology, 2-1-13 Higashiueno, Taito-ku, Tokyo, 110-0015, Japan

Received August 27, 2001. Revised Manuscript Received October 30, 2001

Single-crystal particles of mesoporous niobium−tantalum mixed oxide with a wormhole-like structure were successfully prepared and characterized. The mixed oxide was prepared by a neutral templating method, and the samples provided have thick walls and an unordered pore structure. Neutral block copolymer, $HO(CH_2CH_2O)_{20}(CH_2CH(CH_3)O)_{70}(CH_2CH_2O)_{20}H$, and metal chlorides were used as the template and inorganic source in propanol. The crystallized mesoporous single-crystal structures were obtained by a two-step calcination process; the first calcination process removes the template, forming a mesoporous structure with amorphous wall material, and the second calcination process crystallizes the pore walls while maintaining the mesoporosity. The submicrometer mesoporous particles forming the walls were confirmed by transmission electron microscopy to be single crystals. The pore diameter was found to increase upon crystallization, while retaining the open-pore system. N_2-gas adsorption−desorption analysis indicated that the pore volume of the crystallized sample remained the same as that of the amorphous precursor. The fabricated niobium−tantalum mixed oxide exhibits high thermal, hydrothermal, and mechanical stability.

Introduction

Surfactant templating is the most effective route for the synthesis of mesoporous materials. Ever since the development of MCM-41 (a mesoporous silica) by Mobil researchers,[1] mesoporous material research has focused on silica-based materials.[2−8] Although various applications for mesoporous silicas, such as MCMs[2−4] and FSMs,[5,6] have been suggested because of their uniform pore size and structural ordering, the inherent structural weakness of the material has been an obstructive factor to industrial uses.

The discovery of a neutral templating route for the preparation of mesoporous silica has made it possible to create a material with high structural strength and stability through the formation of a thick-walled structure.[7] In particular, researchers have paid attention to the block copolymers of poly(ethylene oxide) and polypropylene oxide.[8,9] In this synthetic route, an inorganic network is formed by hydrogen bonding, yielding a thick-walled structure with uniform pore size. The lower cost, lower toxicity, and ease of template removal made the use of neutral block copolymers an attractive route.[8]

Recently, the neutral templating route with block copolymers has also been applied in the synthesis of transition metal oxides; titanium, zirconium, aluminum, hafnium, tungsten, tin, niobium, and tantalum oxides.[10,11] Although some of the mesoporous transition metal oxides have turned out to have low pore regularity and uniformity, several metal oxides afford hexagonally ordered mesoporous structures, as confirmed by transmission electron microscopy (TEM) observations. The construction of mesoporous structures of transition metal oxides is anticipated to have specific applications in catalytic reactions,[12] biomaterials,[13] optoelectronics[13] and nanotechnology,[13] by using the higher surface area compared with typical bulk particles and the ability to control the macroscopic morphology.

In general, the mesoporous structure cannot be retained during crystallization, and the structure usu-

* Corresponding author. E-mail: kdomen@res.titech.ac.jp.
† Tokyo Institute of Technology.
‡ Japan Science and Technology.

(1) Kresge, C. T.; Leonowicz, M. E.; Roth, W. J.; Vartuli, J. C.; Beck, J. S. *Nature (London)* **1992,** *359*, 710.
(2) Vartuli, J. C.; Schmitt, K. D.; Kresge, C. T.; Roth, W. J.; Leonowicz, M. E.; McCullen, S. B.; Hellring, S. D.; Beck, J. S.; Schlenker, J. L.; Olsen, D. H.; Sheppard, E. W. *Chem. Mater.* **1994,** *6*, 2317.
(3) Monnier, A.; Schüth, F.; Huo, Q.; Kumar, D.; Margolese, D.; Maxwell, R. S.; Stucky, G. D.; Krishnamurthy, M.; Petroff, P.; Firouzi, A.; Janicke, M.; Chmelka, B. F. *Science* **1993,** *261*, 1299.
(4) Karra, V. R.; Moudrakovski, I. L.; Sayari, A. *J. Porous Mater.* **1996,** *3*, 77.
(5) Yanagisawa, T.; Shimizu, T.; Kuroda, K.; Kato, C. *Bull. Chem. Soc. Jpn.* **1990,** *63*, 988.
(6) Inagaki, S.; Fukushima, Y.; Kuroda, K. *J. Chem. Soc. Chem. Commun.* **1993,** 680.
(7) Tanev, P. T.; Pinnavaia, T. J. *Science* **1995,** *267*, 865.
(8) Bagshaw, S. A.; Prouzet, E.; Pinnavaia, T. J. *Science* **1995,** *269*, 1242.
(9) Zhao, D.; Feng, J.; Huo, Q.; Melosh, N.; Fredrickson, G. H.; Chmelka, B. F.; Stucky, G. D. *Science* **1998,** *279*, 548.
(10) Yang, P.; Zhao, D.; Margolese, D. I.; Chmelka, B. F.; Stucky, G. D. *Nature (London)* **1998,** *396*, 157.
(11) Yang, P.; Zhao, D.; Margolese, D. I.; Chmelka, B. F.; Stucky, G. D. *Chem. Mater.* **1999,** *11*, 2813.
(12) Yue, Y.; Gao, Z. *Chem. Commun.* **2000,** 1755.
(13) Yang, P.; Deng, T.; Zhao, D.; Feng, P.; Pine, D.; Chmelka, B. F.; Whitesides, G. M.; Stucky, G. D. *Science* **1998,** *282*, 2244.

10.1021/cm010775m CCC: $22.00
Published on Web 01/11/2002

ally collapses at the crystallization temperature of the inorganic framework. Despite the difficulty of preparation, mesoporous materials with crystallized wall structures are highly desirable for various applications because of the higher structural strength and the possibility of exploiting the specific properties of the metal oxides themselves. In contrast to the typical mesoporous materials, which form an amorphous wall structure, the existence of nanoparticles within the wall structure of recently prepared metal-oxide materials suggests the possibility of the preparation of novel mesoporous materials with crystallized walls. In the original reports on the preparation of mesoporous transition metal oxides using block copolymer templates, patches of crystallized nanoparticles were formed in the thick wall structure of mesoporous titania and zirconia during calcination for the template removal.[10,11] In the mesoporous titania prepared by a similar method, the nanocrystalline anatase patches were reported to grow by successive hydrothermal treatment before template removal.[12] The presence of crystallized tin oxide has also been reported in a mesoporous tin oxide-silica composite,[14] which exhibited cycling properties as anodes. Recently, the extent of crystallization of mesoporous tungsten oxide films was controlled, and the electrochemical properties of the prepared films were studied.[15] The size of crystalline domains of all these crystallized transition metal oxides was limited to a few nanometers, and each particle is regarded as a polycrystalline, resulting in a ring electron diffraction (ED) pattern.

In our most recent study, we reported that the two-step calcination of a mixture of niobium and tantalum leads to a novel mesoporous metal oxide with a crystallized framework (called NbTa-TIT-1).[16] The particles in this material turned out to be single crystals, confirmed by TEM images and electron diffraction analysis. In this study, we report the physicochemical properties of the crystallized mesoporous materials and discuss the crystallinity and preparation methodology in detail.

Experimental Section

Chemicals. Tri-block copolymer poly(ethylene oxide)-poly(propylene oxide)-poly(ethylene oxide), $HO(CH_2CH_2O)_{20}(CH_2CH(CH_3)O)_{70}(CH_2CH_2O)_{20}H$ (Pluronic P-123) was obtained from BASF, and used as the template. Niobium pentachloride (99.9%, Kojundo Chemical Laboratory Co., Ltd.) and tantalum pentachloride (99.99%, Kojundo Chemical Laboratory Co., Ltd.) were used as the metal sources and as received. Alcohols, methanol, ethanol, butanol, hexanol (Kanto Chemical), and propanol (Wako Pure Chemicals), were used as the solvent.

Synthesis. The synthetic route reported by Yang et al.[10,11] was used with modifications in terms of the solvents and templates used, the metal/template ratio, and promotion of the hydrolysis step by the addition of water, details of which will be reported elsewhere.[17]

In the typical synthesis of crystallized mesoporous niobium−tantalum oxide, 1 g of P-123 is dissolved in 10 g of propanol to prepare a 10 wt % surfactant solution. To this solution is added 0.004 mol of each of $NbCl_5$ and $TaCl_5$ (0.008 mol in total) and the mixture vigorously stirred for 30 min. Subsequently, 1.5 g of distilled water is added and the solution stirred for 10 min to promote hydrolysis. This sol solution is aged at 40 °C in air for 4−7 days to give a gelled product. The crystallization conditions of the mixed oxides are examined for various molar ratios of Nb to Ta: 0:10, 1:9, 3:7, 1:1, 7:3, 9:1, and 10:0.

The amorphous walled precursor of the crystallized mesoporous material is prepared by calcining the gelled product at 400−450 °C for 5 to 20 h in air, yielding an amorphous mesoporous sample with template removed. The sample is then crystallized by further calcination; in the niobium and tantalum mixed oxide with an atomic ratio of Nb:Ta = 1:1 [hereafter referred to as $(Nb,Ta)_2O_5$], the precursor is treated at 650 °C for 1 h in air.

Analyses. Differential thermal analysis (DTA) and thermogravimetry (TG) were performed by using a Shimadzu DTG-50 in air at a heating rate of 5 or 10 °C·min^{-1}. X-ray diffraction (XRD) patterns were obtained on a Rigaku RINT 2100 diffractometer with Cu Kα radiation. The TEM images were obtained with a 200-kV JEOL JEM2010F. Nitrogen-gas adsorption−desorption isotherms were measured by Coulter Omnisorp 100CX and SA-3100 systems, and pore-size distributions were determined by Barrett−Joyner−Halenda (BJH) analysis. Elemental analysis of carbon, hydrogen, and nitrogen was performed on a LECO CHN-932, and chloride was analyzed using a Yanaco SX-Elements Micro Analyzer YS-10.

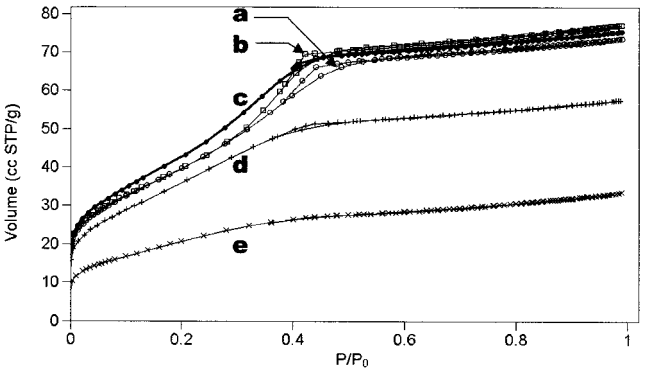

Figure 1. N_2-gas adsorption−desorption isotherms of $(Nb,Ta)_2O_5$ produced with various solvents: (a) methanol, (b) ethanol, (c) propanol, (d) butanol, and (e) hexanol. STP, standard temperature and pressure.

Results and Discussion

1. Solvent Effects. Before crystallization, the preparation of the precursor was examined on the basis of a mixture of equivalent molar amounts of niobium and tantalum oxide [denoted $(Nb,Ta)_2O_5$] as a typical case. Different kinds of alcohols are expected to affect the rate of reaction and condensation. In previous work, ethanol was used for the preparation of mesoporous TiO_2, ZrO_2, SnO_2, WO_3, Nb_2O_5, and Ta_2O_5, whereas butanol was used as the solvent for HfO_2 synthesis.[11] In this study, five $(Nb,Ta)_2O_5$ samples were prepared by using different alcohol solvents. The N_2-gas adsorption−desorption isotherms of those samples are compared in Figure 1. Type IV isotherm curves[18] are observed for samples prepared in methanol, ethanol, and propanol. The increase in the adsorbed N_2 volume plateaued at 0.4−0.5 relative pressure (P/P_0), indicating saturation of the mesoporous structure of the samples. In contrast, the samples prepared in butanol and hexanol exhibited poorer mesoporosity, lower surface area, and smaller pore volume (Table 1). Therefore, butanol and hexanol are regarded as unsuitable solvents for the synthesis of the mesoporous materials dealt with in this study.

(14) Chen, F.; Shi, Z.; Liu, M. *Chem. Commun.* **2000,** 2095.
(15) Chen, W.; Baudrin, E.; Dunn, B.; Zink, J. I. *J. Mater. Chem.* **2001,** *11*, 92.
(16) Lee, B.; Lu, D.; Kondo, J. N.; Domen, K. *Chem. Commun.* **2001,** 2118.
(17) Katou, T.; Lee, B.; Lu, D.; Kondo, J. N.; Domen, K., manuscript in preparation.

Table 1. Mesoporosity of $(Nb,Ta)_2O_5$ Prepared with Various Solvents

solvent	BET surface area[a] ($m^2 \cdot g^{-1}$)	mean pore size[b] (nm)	pore volume[c] (mL g^{-1})
methanol	154	3	0.12
ethanol	153	3	0.14
propanol	168	3	0.12
butanol	140	2.5	0.08
hexanol	78	–	–

[a] Crystallinity of the particles was confirmed by the electron diffraction patterns, which were collected from 50 particles in a few-hundred-nanometer size. [b] The pore size is estimated from the BJH analysis in adsorption branch of the N_2 sorption isotherm. [c] The pore volume is measured from 2 to 50 nm of the pore-size distribution.

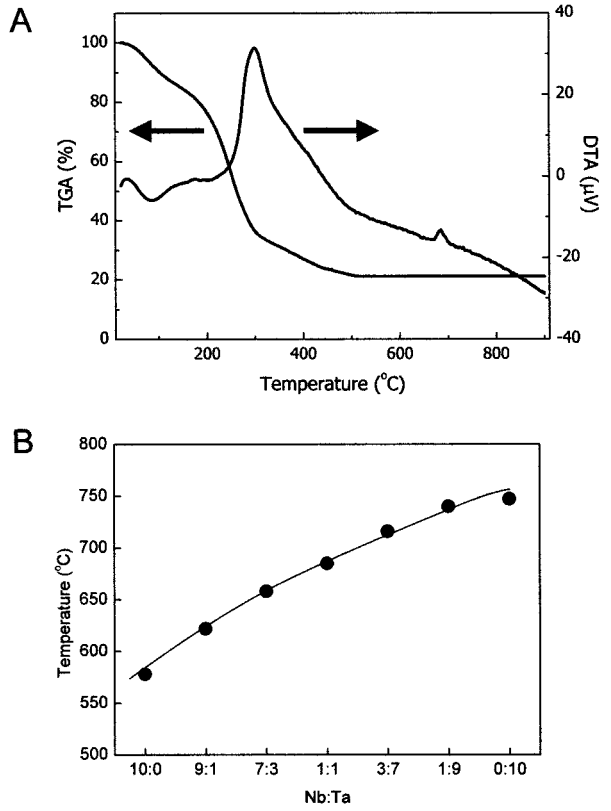

Figure 2. (A) TG/DTA analysis of $(Nb,Ta)_2O_5$ sample; (B) DTA peaks of several niobium and tantalum ratios.

The desorption branches in the isotherms of the samples prepared in methanol, ethanol, and propanol are analogous to H2-type hysteresis, which is an indicator of a three-dimensionally interconnected or ink-bottle porous structure.[18] However, the degree of hysteresis is significantly lower than that of typical three-dimensionally interconnected or ink-bottle porous materials. Minor hysteresis is also observed for a mesoporous silica with wormhole-like mesoporosity prepared with a neutral template.[19,20] The niobium and tantalum mixed oxide materials prepared here are thus considered to possess such a wormhole-like mesoporous structure. This is observed directly by TEM, as detailed below.

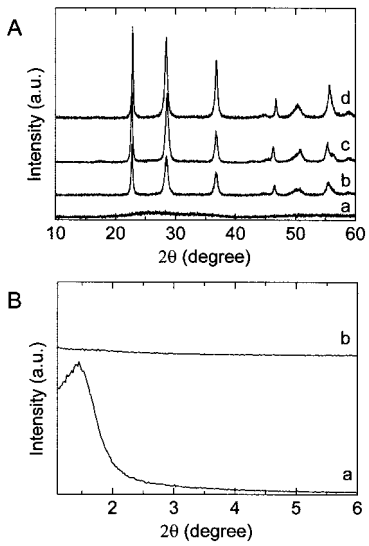

Figure 3. (A) Wide-angle and (B) low-angle XRD patterns of the precursor (curve a) and the crystallized sample (curve b). Crystallized niobium oxide (curve c) and tantalum oxide (curve d) are shown for comparison.

Of the alcohol solvents examined, propanol produced the sample with highest Brunauer–Emmett–Teller (adsorption isotherm) (BET) surface area and smallest hysteresis loop (Table 1). Therefore, in niobium and tantalum mixed oxide, propanol was chosen as the most suitable solvent.

2. Crystallization Conditions for Mixed Oxides. The absence of chloride in as-synthesized samples, as determined by elemental analysis, confirms that the hydrolysis of the metal oxide framework was complete. TG/DTA results for the as-synthesized $(Nb,Ta)_2O_5$ are shown in Figure 2A. The TG curve of the as-synthesized $(Nb,Ta)_2O_5$ indicates that the template is completely eliminated at 400–500 °C (Figure 2A). The removal of the template by calcination results in the appearance of an exothermic peak at around 300 °C in the DTA curve. Elemental analysis of the sample treated to above 400 °C revealed less than 0.1 wt % carbon, which is within experimental error. This result is further evidence that the template is completely removed by treatment at temperatures greater than 400 °C. In the 650–700 °C region, another exothermic peak emerges without a corresponding weight loss, suggesting that crystallization of the $(Nb,Ta)_2O_5$ sample occurs at temperatures exceeding 650 °C.

The crystallization temperatures of seven different as-synthesized samples with various molar ratios of Nb to Ta are compared in Figure 2B, where the DTA peak at above 500 °C is plotted for each sample. The crystallization temperatures of niobium oxide (575 °C) and tantalum oxide (745 °C) agree well with those for nonporous materials,[21] and increase with the Ta ratio. The gradual and continuous change in crystallization temperature is indicative of the homogeneous mixing of the two metal oxides.

The crystallized mixed oxide sample exhibited the same mesoporosity even though pure niobium or tantalum oxide loses all mesoporosity after crystallization.

(18) Lowell, S.; Shields, J. E. *Adsorption by Powders and Porous Solids. Principles, Methodology and Applications*; Academic Press: San Diego, 1999.
(19) Prouzet, E.; Pinnavaia, T. J. *Angew. Chem., Int. Ed. Engl.* **1997,** *36*, 516.
(20) Kim, S.-S.; Pauly, T. R.; Pinnavaia, T. J. *Chem. Commun.* **2000,** 835.
(21) Holtzberg, F.; Reisman, A.; Berry, M.; Berkenblit, M. *J. Am. Chem. Soc.* **1957,** *79*, 2039.

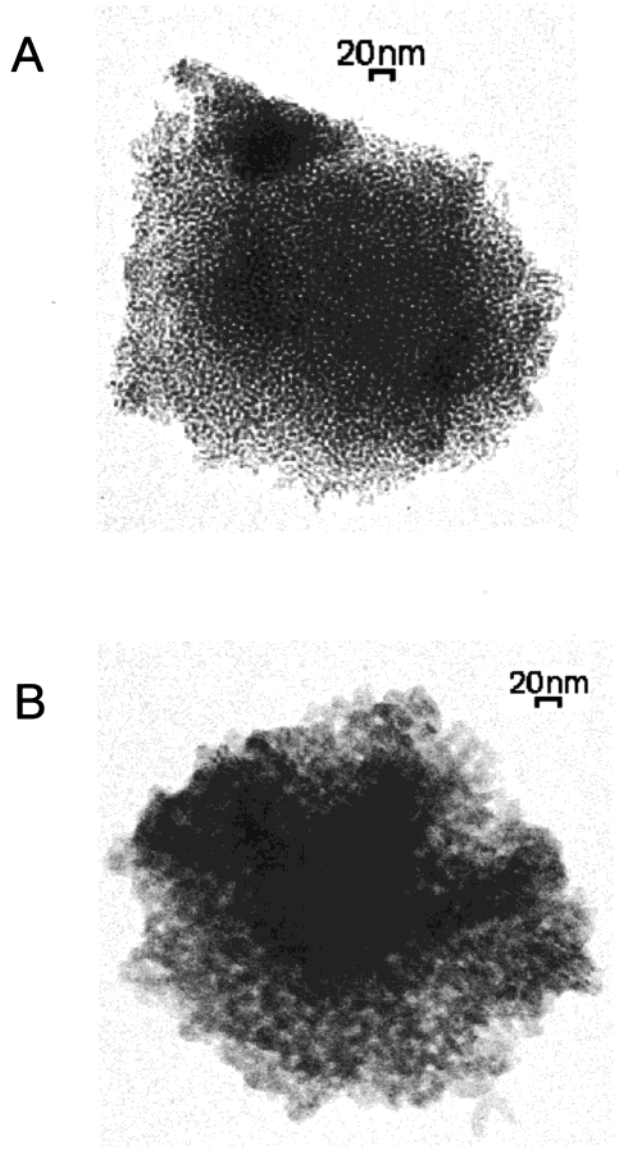

Figure 4. TEM images of (A) the amorphous precursor and (B) the crystallized sample.

Table 2. XRD Data of Pure Niobium, Tantalum and Mesoporous Niobium and Tantalum Mixed Oxides

Nb_2O_5[23]			Ta_2O_5[24]			$(Nb,Ta)_2O_5$	
d (Å)	2*θ* (deg)	hkl	*d* (Å)	2*θ* (deg)	hkl	*d* (Å)	2*θ* (deg)
5.22	16.985	1 3 0	5.0362	17.596	0 8 0	5.22	16.94
3.93	22.625	0 0 1	3.8880	22.854	0 0 1	3.89	22.80
3.15	28.332	1 8 0	3.1532	28.279	1 11 0	3.13	28.46
3.09	28.894	2 0 0	3.0990	28.785	2 0 0	3.08	28.94
2.460	36.525	1 8 1	2.4490	36.665	1 11 1	2.44	36.88
2.428	37.024	2 0 1	2.4233	37.068	2 0 1	2.42	37.06
2.017	44.94	2 11 0	2.0063	45.155	1 19 0	2.01	44.92
1.969	46.233	0 0 2	1.9440	48.687	3 7 0	1.95	46.50
1.832	49.770	0 16 0	1.8313	49.747	1 21 0	1.81	50.34
1.793	50.929	3 8 0	1.7994	50.690	3 11 0	1.80	50.66
1.669	55.019	1 8 2	1.6548	55.484	1 11 2	1.65	55.50
1.660	55.343	1 17 0	1.6468	55.777	2 0 2		
1.659	55.379	2 0 2	1.6330	56.289	3 11 1	1.63	56.18
1.632	55.376	3 8 1	1.5766	58.493	2 22 0	1.57	58.72

The relatively lower crystallization temperature of $(Nb,Ta)_2O_5$ is thought to allow some of the original mesoporosity to be retained during crystallization.

3. Single-Crystal Mesoporous Particles. The crystallized $(Nb,Ta)_2O_5$ sample was then characterized in detail. The XRD patterns of $(Nb,Ta)_2O_5$ before and after crystallization are shown in Figure 3A. No peaks were observed in the XRD pattern of the $(Nb,Ta)_2O_5$ after initial calcination (pattern a), indicating that at this stage, the walls were amorphous. After the second calcination process, the sample has a clear crystal (pattern b). The XRD peaks of the crystallized sample are difficult to identify precisely because they correspond to neither niobium oxide nor tantalum oxide.[22] In Table 2, specific XRD peaks of $(Nb,Ta)_2O_5$ are listed together with those for the low-temperature phase of Nb_2O_5 [23] and Ta_2O_5.[24] The *d* values of $(Nb,Ta)_2O_5$ do not correspond exactly to Nb_2O_5 or Ta_2O_5, which have a similar orthorhombic structure (Figure 3A, curves c and d). The three main peaks for $(Nb,Ta)_2O_5$ occur between (001), (180), and (181) of Nb_2O_5 and (001), (1 11 0), and (1 11 1) of Ta_2O_5. Therefore, $(Nb,Ta)_2O_5$ is considered to have an orthorhombic wall structure. As the DTA result showed, rather than being a physical mixture, niobium and tantalum oxide exist as a mixed oxide in solid solution. The homogeneous mixture of niobium and tantalum was also confirmed by elemental analysis with a scanning electron microscope. From an energy-dispersive X-ray analysis using the TEM apparatus, the atomic ratio of niobium to tantalum was found to be 1:1 in all regions (<5 nm in diameter region) of the sample.

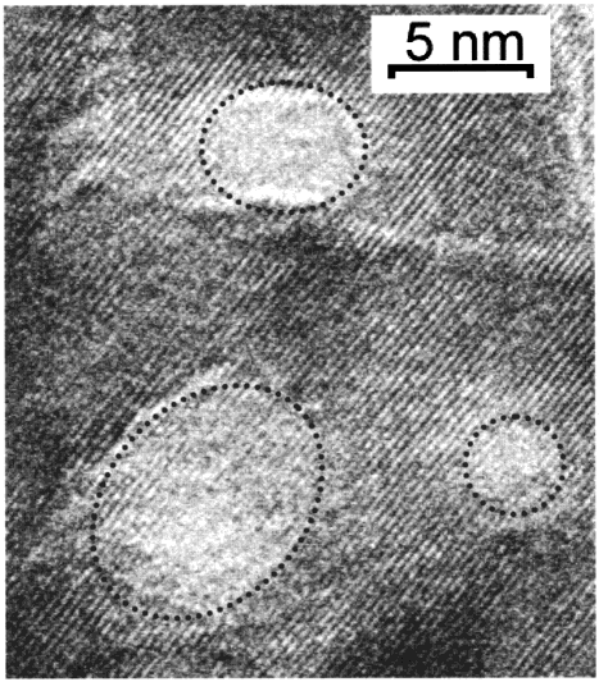

Figure 5. High-resolution TEM image of crystallized $(Nb,Ta)_2O_5$ sample.

Low-angle XRD patterns of the precursor and the crystallized sample are shown in Figure 3B. At around 1.5 deg, there is a broad (100) peak for the amorphous

(22) Reisman, A.; Holtberg, F. *High-Temperature Oxides, Part II. Oxides of Rare Earths, Titanium, Zirconium, Hafnium, Niobium and Tantalum*; Alper, A. M., Ed.; Academic Press: New York, 1970; Chapter 7.
(23) Waring, J. L.; Roth, R. S.; Parker, H. S. *J. Res. Natl. Bur. Stand., Sect. A* **1973,** *77A*, 705.
(24) Stephenson, N. C.; Roth, R. S. *Acta Crystallogr., Sect. B* **1971,** *27*, 1037.
(25) Sinclare, R. *Treatise on Materials Science and Technology, Properties and Microstructure*; MacCrone, R. K., Ed.; Academic Press: New York, 1977; Vol. 11, Chapter 1.

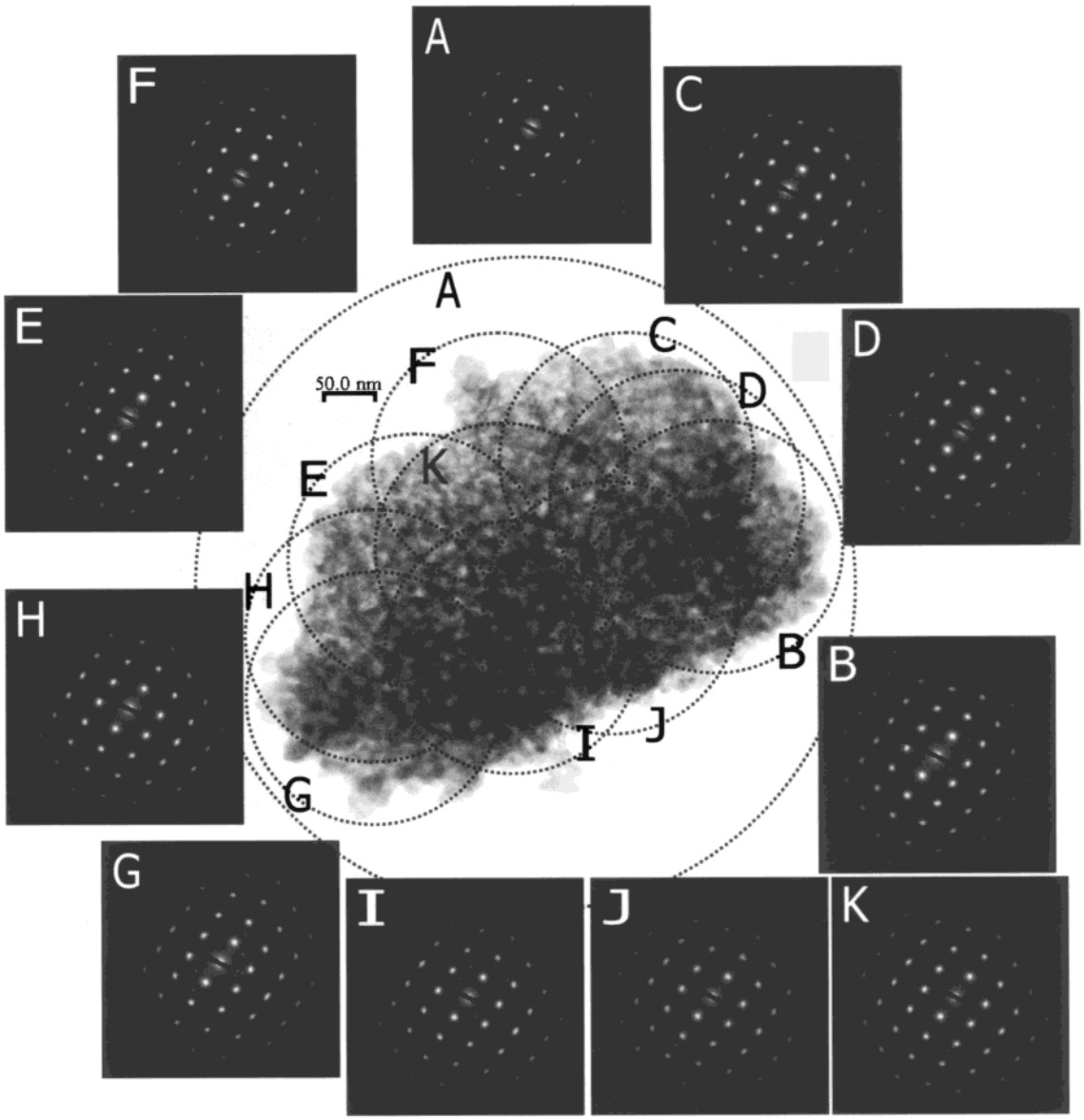

Figure 6. Electron diffraction of crystallized mesoporous sample obtained for whole particle (pattern A) and local areas (patterns B−K).

precursor (Figure 3B, pattern a). This result is in good agreement with that for mesoporous silica prepared by using a neutral template,[20] suggestive of a wormhole-like unordered mesoporous structure. The peak in the low-angle region disappeared after crystallization (Figure 3B, pattern b). This not to the collapse of the mesopores, but rather is attributed to pore expansion upon crystallization, as shown below. When the pore diameter expanded to greater than 10 nm in the thick-walled structure, a (100) peak appears at less than 0.5 deg, which is beyond the limit of our observations.

A TEM image of $(Nb,Ta)_2O_5$ before crystallization is shown in Figure 4A. At this stage, the sample has a uniform open-pore structure of 3- to 4-nm-diameter pores in an unordered array. This observation agrees well with the N_2-gas adsorption−desorption result (Figure 1, curve c). From a comparison of the TEM images of $(Nb,Ta)_2O_5$ before and after crystallization, there is a distinct increase in pore size after crystallization (Figure 4B). Even after crystallization, however, the open-pore system is retained. The structure of the pore walls was confirmed in a high-resolution lattice image (Figure 5). After crystallization, the distribution in pore size becomes broader, as evidenced by the observation of a wide range of pore sizes in the image. The lattice image was taken in the same place. This lattice pattern is consistent throughout the wall structure, with little irregularity, indicating that the pores do not occur as voids between crystals, but are contained within single particles.

We also captured 12 images around the edge of a particle (ca. 0.2 μm in diameter) at high resolution, and confirmed that the lattice fringes of particles were uniform throughout the wall structure. Because the fringe pattern in the observed regions did not vary, we conclude that the mesoporous particle was a single crystal.

The crystallinity of the particle was evaluated by ED measurements. The ED patterns obtained for a whole particle and 10 positions in a 500-nm range are shown in Figure 6. If the particle was partly amorphous or an aggregate of smaller particles, the ED patterns would

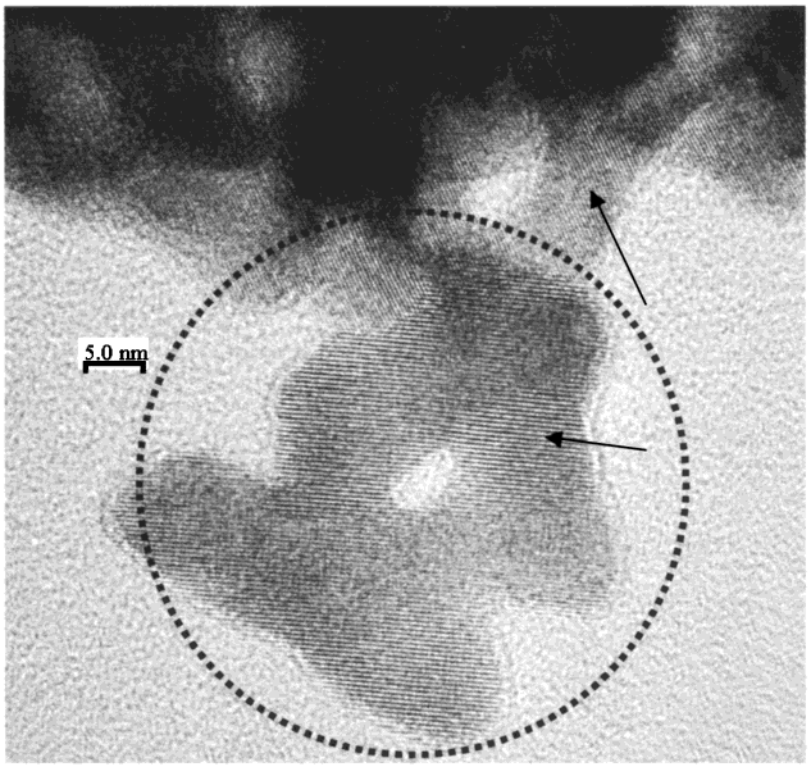

Figure 7. Small fragment on crystalline particle. Direction of lattice fringe differs from that of the crystalline particle.

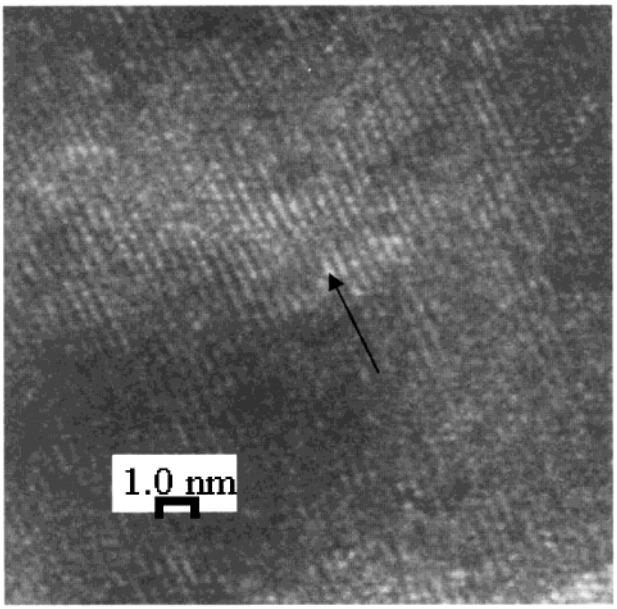

Figure 8. Distortion in local lattice-fringe image at high resolution.

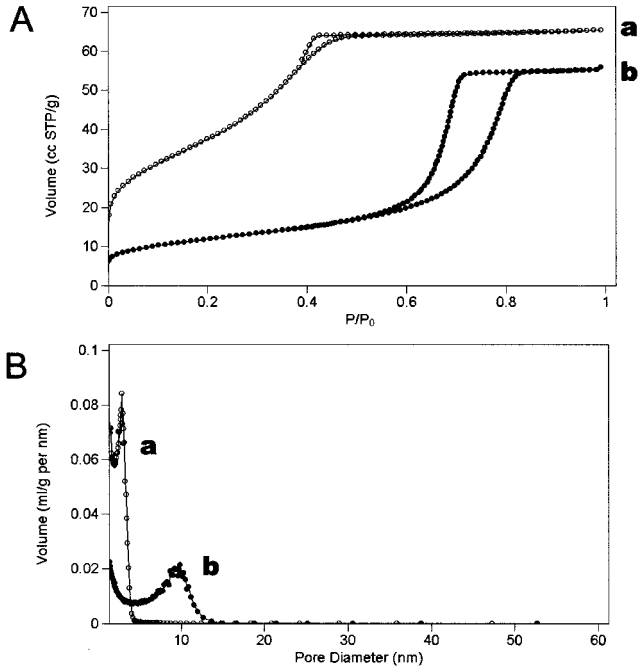

Figure 9. (A) N_2-gas adsorption−desorption isotherms and (B) pore-size distribution of (a) the precursor and (b) the crystallized sample. Pore-size distribution was calculated by BJH analysis (adsorption branch).

be distorted and inconsistent. However, all ED patterns obtained for the particle are identical, confirming that the particle is uniformly crystallized. Indeed, the spot pattern indicates that this particle is a single crystal. A few weak spots were observed in some ED patterns (e.g., patterns G and I), attributable to small fragments on the surface of the particle. The high-resolution image in Figure 7 shows such a fragment, indicated by a dotted circle. The lattice fringes of this fragment are oriented in a different direction from those of the main particle. Therefore, the particles of crystallized $(Nb,Ta)_2O_5$ are considered to be mesoporous single crystals. We call this type of crystallized material with a wormhole-like mesoporous structure TIT-1.[16] In the present case, the mixture of niobium and tantalum oxide is indicated by the prefix NbTa, i.e., NbTa-TIT-1.

Although fringe distortions and point defects were observed (see Figure 8), no antiphase boundaries, disordered fringe periodicity or rotational domain boundaries were found.[25] Of the 50 particles with several hundreds of nanometers to submicrometer diameter sizes selected for ED analysis, more than 90% were

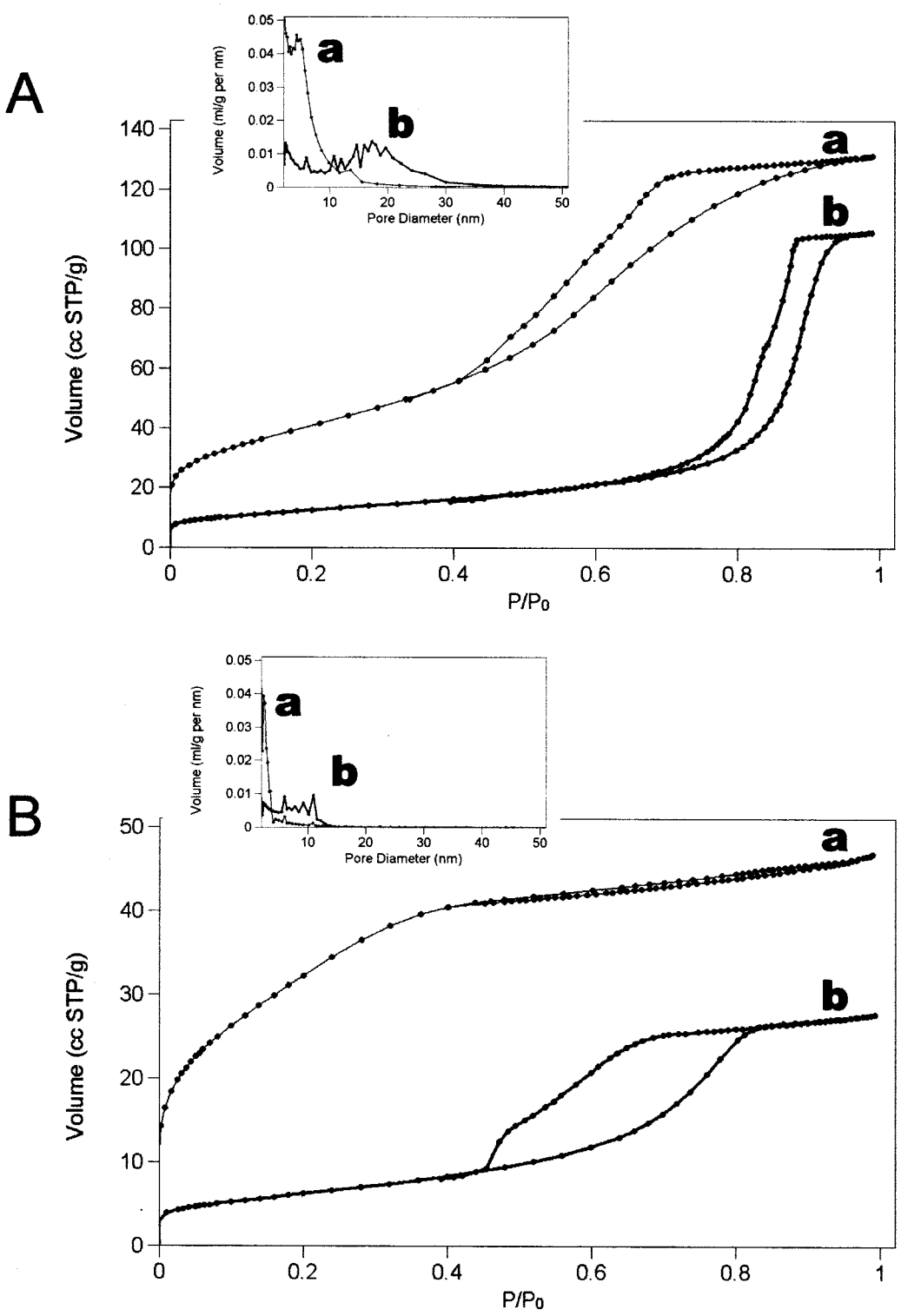

Figure 10. N_2-gas adsorption−desorption isotherms and BJH pore-size distribution (insets) of amorphous (a) and crystallized mesoporous (b) niobium oxide (A) and tantalum oxide (B).

confirmed to be crystallized; only 10% were insufficiently crystallized under the present calcination conditions of 650 °C for 1 h.

As the TEM images show only small regions, the overall mesoporosity of the sample was examined by N_2-gas adsorption−desorption analysis. Isotherms of $(Nb,Ta)_2O_5$ before and after crystallization are shown in Figure 9A. Although the adsorption volume for the amorphous precursor saturates at 0.4−0.5 P/P_0 (curve a), the crystallized sample (NbTa-TIT-1) continues to adsorb N_2 up to 0.6−0.8 P/P_0 (curve b). This result is indicative of an increase in the pore size. After crystallization, the BET surface area of the examined sample decreased from 170 to 50 $m^2 \cdot g^{-1}$ (Table 3). A BJH analysis of the adsorption curve revealed that the pore size increases from 3 to 4 nm to 10 nm after crystallization. (Figure 9B)

A niobium and tantalum oxide sample with compositional ratio Nb:Ta = 7:3 [NbTa (7:3)-TIT-1] had a similar isotherm curve, with an unordered mesoporous

Table 3. Calcination Time Effect of the Crystallized $(Nb,Ta)_2O_5$ Sample

second step calcination	crystallinity[a] (%)	pore size[b] (nm)	BET surface area ($m^2\ g^{-1}$)	pore volume[c] (mL g^{-1})
none	0	3	168	0.12
650 °C for 10 min	20	3	94	0.08
650 °C for 30 min	80	6	71	0.12
650 °C for 60 min	90	10	48	0.12
650 °C for 10 h	100	10−20	23.9	0.11
650 °C for 20 h	100	22−32	22.2	0.14

[a] Crystallinity of the particles was confirmed by the electron diffraction patterns, which were collected from 50 particles in a few-hundred-nanometer size. [b] The pore size is estimated from the BJH analysis in adsorption branch of the N_2 sorption isotherm. [c] The pore volume is measured from 2 to 50 nm of the pore-size distribution.

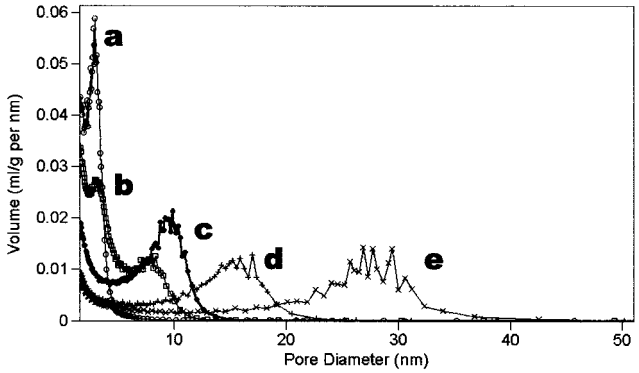

Figure 11. BJH pore-size distributions of $(Nb,Ta)_2O_5$ sample calcined at 650 °C for (a) 10 min, (b) 30 min, (c) 60 min, (d) 10 h, and (e) 20 h.

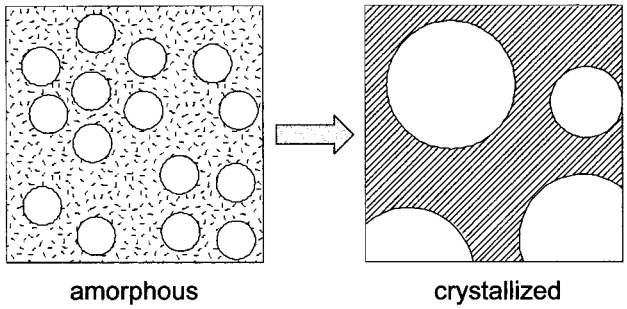

Figure 12. Model of pore-size expansion.

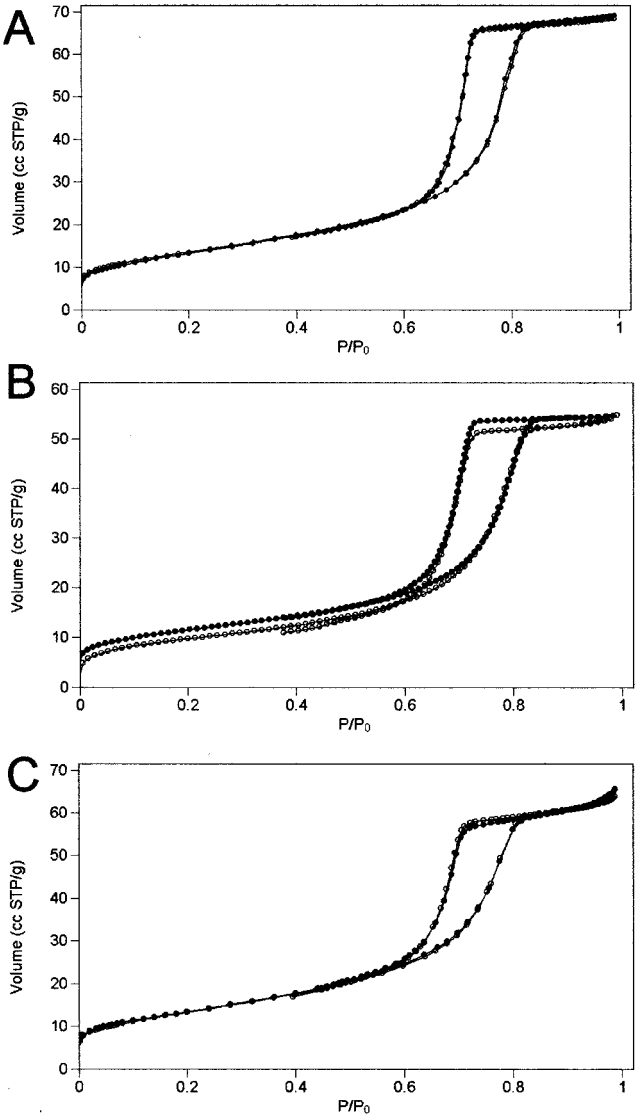

Figure 13. (A) Thermal, (B) hydrothermal, and (C) mechanical stability of the crystallized sample. Isotherm curves (○) before and (●) after treatment. Thermal stability was tested by pressing the sample at 500 °C for 10 h. Hydrothermal stability was tested by treating the sample at 200 °C and 15 atm for 24 h. Mechanical strength was tested by subjecting the sample to 500 kg·cm^{-2} for 17 h.

structure and pore diameter of 10 nm. Mesoporous materials with relatively large pores were synthesized by crystallization in all ratios examined.

4. Crystallization of Mesoporous Niobium or Tantalum Oxide. The formation of crystallized wall structures in pure mesoporous niobium or tantalum oxide was also examined. After calcination at 400 °C for 20 h, mesoporous niobium and tantalum oxides were obtained with amorphous wall structures. The samples were further calcined under the previous crystallization conditions. From DTA results (Figure 2B), the crystallization conditions for the amorphous precursors of mesoporous niobium and tantalum oxides were chosen as 600 and 750 °C for 1 h, respectively.

The N_2-gas adsorption−desorption isotherms of mesoporous niobium (Figure 10A, curve a) and tantalum oxide (Figure 10B, curve a) after initial calcination (amorphous wall) are type IV isotherms. After crystallization, the uptake of N_2 shifted to higher P/P_0 for both niobium (Figure 10A, curve b) and tantalum (Figure 10B, curve b) oxides. The hysteresis loop of the isotherm for crystallized niobium oxide is a typical H1-type isotherm, indicating the presence of tubular pores. The tantalum oxide sample exhibited H2-type isotherms, indicative of a three-dimensionally interconnected or ink-bottle porous structure. The BET surface area after crystallization decreased from 150 to 45 $m^2 \cdot g^{-1}$ and from 120 to 23 $m^2 \cdot g^{-1}$ in the niobium oxide and tantalum oxide samples. Furthermore, the broad pore-size distributions suggest poorer regularity of porous structure than the mixed oxide samples. In the niobium oxide sample, particles were poorly crystallized according to TEM observations, and pores occurred as voids between particles. The crystallized tantalum oxide also had poor mesoporosity. Mixing two components is therefore effective for the synthesis of crystallized mesoporous oxides.

5. Pore-Size Expansion by Calcination. The BJH analysis for pore-size distribution indicates that the pore diameter increased in the second calcination process (Figure 9B). This was investigated in detail by examining samples subjected to different periods of crystallizing calcination at 650 °C. The BJH analysis reveals that the sample calcined for 10 min (Figure 11, curve a) has a pore size similar to the amorphous precursor. After 30 min, 8-nm pores appeared in the distribution whereas the tail down to 3 nm remained. The change in pore size corresponded to the progress of crystallization according to TEM-ED analysis; only 20% of the particles were crystallized after 10 min, whereas 80% of the particles were crystallized after calcination for 30 min (Table 3). The crystallinity of the samples was estimated from TEM observations of 50 particles. After 1 h, the smaller pores have clearly disappeared and larger pores of 10 nm in diameter are observed. This represents a rapid pore expansion with calcination. The pore expansion continued with crystallization until the mesoporous structure collapsed after 10 h. The BJH analysis of samples calcined for 10 h reveals an extremely broad pore-size distribution.

In general, when mesoporous metal oxides are treated at greater than the crystallization temperature, the pore walls collapse and bulk particles without pores remain. However, thick-walled structures remain stable even at relatively high temperatures. The high thermal stability of silica-based SBA-15[9] is attributed to such a thick-walled structure. Mixing Nb and Ta lowers the crystallization temperature from that for pure tantalum oxide, and the relatively low surface tension of niobium oxide is also thought to be an important factor.[26] The homogeneous mixing of niobium oxide and tantalum oxide without phase separation is possible because of the similar properties of the two materials. The mesoporous mixed oxide, NbTa-TIT-1, is metastable, and further thermal treatment at the crystallization temperature transforms it to bulk particles as above. From a comparison of TEM images before and after crystallization (Figure 4), a schematic model for pore expansion has been constructed. In the model, several small pores of the precursor merge to form one larger pore during crystallization (Figure 12). This explains the broadening of the pore-size distribution. Nevertheless, mesoporosity is retained and the pore volume remained almost unchanged after crystallization (Table 3). This model is currently being verified by in-situ TEM analysis of the crystallization process at higher temperatures.

6. Thermal and Hydrothermal Stability and Mechanical Strength. The NbTa-TIT-1 sample exhibits higher thermal and hydrothermal stability and mechanical strength than mesoporous materials with amorphous walls. After several treatments, the samples were characterized by N_2-gas adsorption−desorption isotherm measurements. Thermal and hydrothermal treatments were performed at 500 °C for 10 h in air, and at 200 °C and 15 atm for 1 day, respectively. As compared in Figure 13A,B with the NbTa-TIT-1 before treatment, no significant change occurred after either treatment. The NbTa-TIT-1 sample also remained unchanged after being pressed mechanically at 500 kg·cm^{-2} for 17 h (Figure 13C). NbTa-TIT-1, a crystallized mesoporous transition metal oxide, is expected to be very useful in a range of applications.

Conclusion

Mesoporous niobium−tantalum mixed oxide was prepared by a neutral block copolymer templating method. The two-step calcination of the mixed oxide effectively crystallized the samples while retaining the mesoporosity. TEM and ED observations verified the mesoporous structure and single-crystal composition of the sample. Despite the pore-size expansion, the pore volume remained unchanged after crystallization. The material was shown to have outstanding stability under severe conditions, and as such is expected have a range of possible applications.

Acknowledgment. This work was supported by the Core Research for Evolutional Science and Technology (CREST) program of the Japan Science and Technology (JST) Corporation.

CM010775M

(26) Nair, P.; Nair, J.; Raj, A.; Maeda, K.; Mizulami, F.; Okubo, T.; Imitsu, H. *Mater. Res. Bull.* **1999,** *34*, 3.